Fatigue Strength For Shallow Defects Under Torsion

Stefano Beretta[1,a], K. Valiullin[1,b]

[1]Politecnico di Milano, Department of Mechanical Engineering, Via La Masa 34, 20156 Milano Italy

[a]stefano.beretta@polimi.it, [b]khaydar.valiullin@mecc.polimi.it

Keywords: torsion fatigue, short cracks, Mode I, Mode III, thresholds.

Abstract. Fatigue strength in presence of inhomogeneities is controlled by the threshold condition of small cracks which nucleate at the defect tip. In biaxial in-phase fatigue strength is controlled by the threshold condition of small cracks at Mode I branches. This paper presents the results of different sets of torsion fatigue tests which use shallow micronotches on a SAE 5135 gear steel. The results show that fatigue strength is controlled by the competition between Mode I and Mode III propagation even when the failure mode is Mode I.

Introduction

Fatigue strength in the presence of inhomogeneities is controlled by the threshold condition of small cracks which nucleate at the defect tip. Therefore, the fatigue limit is associated with the threshold condition of small cracks [1]. In the case of torsion fatigue it has been shown that for round defects the fatigue strength under bi-axial loading is controlled by the presence of mode I small cracks, whose threshold condition is a function of stress bi-axiality [2]. In accordance with this concept, fatigue limit under torsion loading, in presence of surface spherical defects, is approximately 85% of the fatigue limit under tension as it has been found by Endo [3] for cast iron. It therefore follows that if the threshold condition of small cracks under torsion is characterized by the formation of Mode I branches, fatigue strength can then be predicted by knowing the relationship between Mode I ΔK_{th} and crack size (as it was shown by Murakami & Takahashi [4]). However, some mechanical components subjected to torsion (e.g. automotive half-shafts) show fatigue failures characterized by shear crack propagation triggered by shallow longitudinal defects [5].

Torsional tests in presence of shallow defects

Material. The material analysed is a quenched and tempered SAE 5135 gear steel (UTS= 2100 MPa, yield strength = 1480 MPa; cyclic 0.2% proof stress = 850 MPa), which was subjected to a series of bending fatigue test, at R= -1 onto micronotched specimens, in order to determine the relationship between fatigue strength and defect size (see Fig.1). Since it was possible to observe non-propagating cracks in the tip of run out specimens, fatigue limit test results allows us to obtain a relationship of the type [5] (where parameter $\sqrt{area_o}$ was found by interpolating fatigue limit test results):

$$\Delta K_{th} = \Delta K_{th,LC} \cdot \sqrt{\frac{\sqrt{area}}{\sqrt{area} + \sqrt{area_o}}} \quad (1)$$

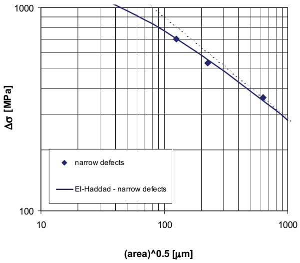

a)

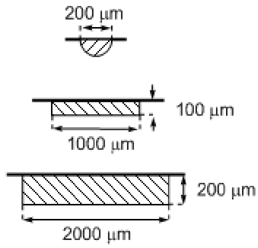

b)

Fig.1. Fatigue tests on gear steel: a) threshold model for fatigue strength of SAE 5135 at R=-1; b) micronotches adopted in bending tests

Torsion fatigue tests. Similar experiments were carried out under torsion with longitudinal and transverse shallow micronotches, see Fig. 2.


a)

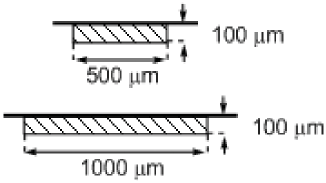

b)

Fig.2. Torsion fatigue tests on gear steel: a) equipment for torsion test; b) micronotches adopted in torsion tests specimen

Results of the fatigue limit tests in alternating torsion (at stress ratio R= -1) are shown in Tab. 1. It is interesting to note that the ratio τ_w/σ_w is completely different from the typical value for round defects [4, 6]. The observation of two run outs specimens, after breaking them in liquid nitrogen, showed that, below τ_w there is the formation of longitudinal non propagating Mode III shear cracks at the bottom of the micronotch (in the central part) in the order of 20 µm (see Fig. 4), which form branches at 45° (towards the end of the defect). Failures occur on fracture planes at 45° which coincide with the non propagating branches, see Fig. 3.

Table 1. Torsion tests on gear steel

Micronotch type [length x depth]	√area [µm]	$\Delta\tau_w$ [MPa]	τ_w/σ_w
500×100 [µm]	225	660	1.2
1000×100 [µm]	330	630	1.3

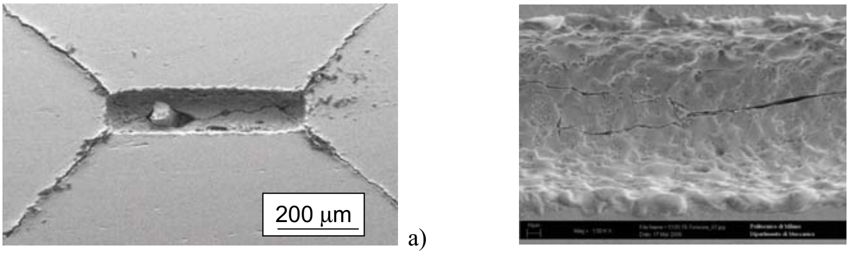

a) b)

Fig.3. Fractography of torsion tests on gear steel: a) broken specimen with a 500×100 μm micronotch; b) non propagating shear cracks at the bottom of the 1000x100 μm micronotch of run out specimen (τ_a= 310MPa, N= 12x10^6 cycles)

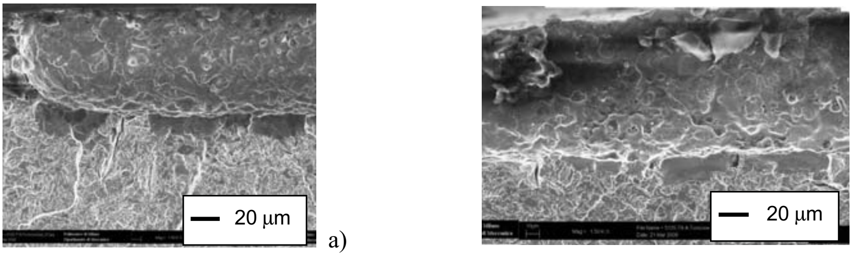

a) b)

Fig.4. Torsion test run out specimen SEM images of Mode III non propagating cracks 20 μm deep: a) micronotch 500x100 μm, N= 12x10^6 cycles at τ_a= 330MPa, b) micronotch 1000x100 μm, N= 12x10^6 cycles at τ_a= 310MPa

Finite element modeling results

The FEA (finite element analysis) were carried out by means of the general purpose commercial software ABAQUS® [7]. The cracks emanating from the two types of the shallow defect adopted in the torsion fatigue tests were modeled by means of FEM (finite element modeling), the cracks were assumed to be modeled in the rectangular form, see Fig.5. The results were analyzed in terms of SIF (stress intensity factor) and geometric factors of the crack, and then compared with the analytical solutions of Sih & Kassir, which have been proved to be satisfactory also for semi-elliptical surface cracks [8], and bi-dimensional SIF solutions for edge cracks were also considered.

FEA showed that in the case of the 500x100 μm micronotch the geometric factor of the crack is not far from the Sih & Kassir solution with the increase of the depth of the crack, while for 1000x100 μm micronotch geometric factor solution tends to the bi-dimensional solution, see Fig. 6.

It can be seen also that the Mode III SIF remains almost constant along the crack front: in particular for approximately 60% of the defect length the ratio K_{III} and $K_{III,\,max}$ remains in the interval of $0.9 \leq K_{III}/K_{III,\,max} \leq 1$.

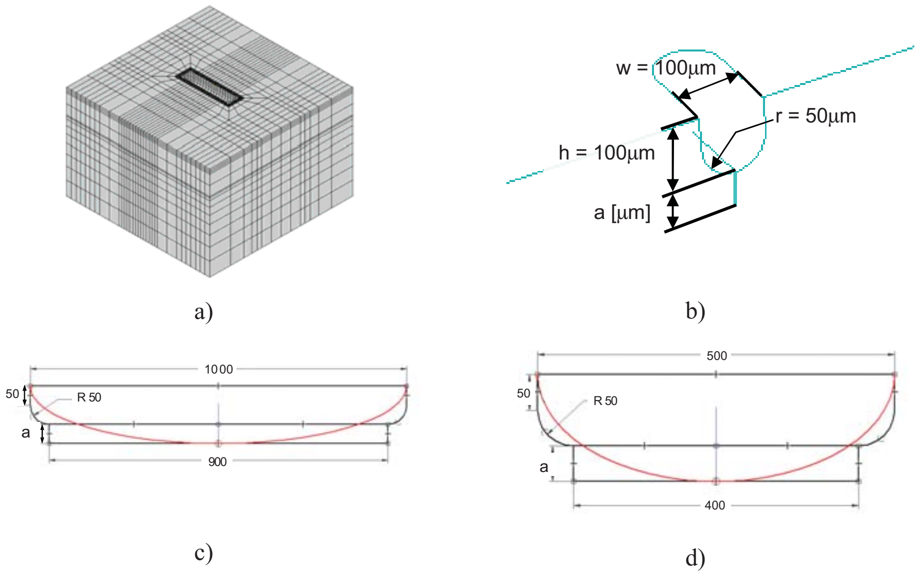

Fig.5. Finite element model of: a) 500x100 micronotch; b) rectangular crack emanating from the micronotch; c), d) Sih & Kassir approximation for semi-elliptic crack

.

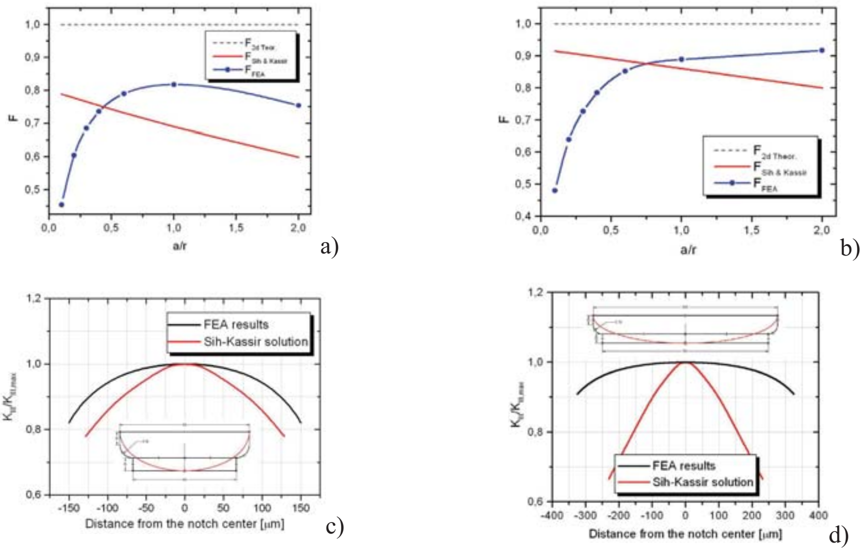

Fig.6. FEA results comparison with analytical solutions: a), b) geometric factor solutions, micronotch length a) 500 µm, b) 1000 µm; c), d) SIF normalized by $K_{III,\, max}$ along the 50 µm deep crack, micronotch length c)500 µm, d) 1000 µm

Analysis

Mode I branch facets. Analyzing the fracture mechanism, it can be said that the torsion fatigue limit coincides with the threshold condition for propagation of Mode I branches. When a crack is loaded in Mode III, according to Pook [9], propagation should occur onto tilted planes with an angle θ so that:

$$\tan 2\theta = \frac{2K_{III}}{K_I(1-2\nu)} \tag{2}$$

onto these planes K_θ is:

$$K_\theta = 0.5[(K_I(1+2\nu)+[K_I^2(1-2\nu)^2+4K_{III}^2]^{0.5}] \tag{3}$$

Since in our case K_I is equal to zero, θ = 45° we can say that $K_\theta = K_{III}$.
In fact, if we will take the results of the torsion fatigue tests and imagine the existence of the minimum 20 μm crack in the micronotch tip of the each specimen we can calculate Mode III SIF for each shear longitudinal cracks at the tip of micronotches with geometric factor found by FEA. Plotting obtained SIF for each specimen (under the hypothesis of 20 μm crack) on the Kitagawa diagram it was possible to observe that torsion fatigue strength corresponds to ΔK_{th} on prospective facets at 45°. On the other hand, by adopting the same method it was possible to obtain very good predictions of τ_w.

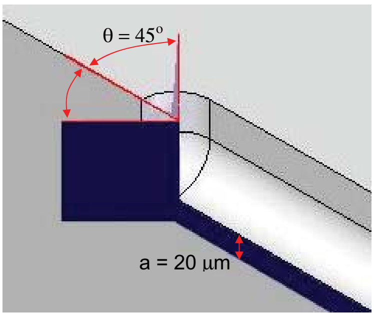

a)

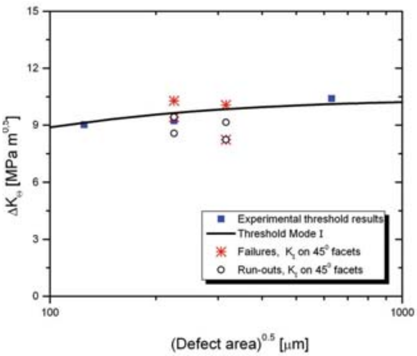

b)

Fig.7. Estimation of the fatigue strength under torsion: a) threshold mechanism for fatigue strength under torsion, b) K_θ onto Mode I facets ahead of a 20 μm crack

Mode III non propagating cracks. Taking run out specimens of torsion fatigue tests with longitudinal defects, loaded at stress levels close to fatigue limit, transverse sections of the micronotches were cut and polishe. The results of the sectioning showed that non propagating cracks in this case were more deep than the first evidence of 20 μm, see Fig. 8 a. It was possible to reconstruct whole crack front by sectioning the specimen along the micronotch length with steps of 50 μm: the results of approximate crack front are shown in the Fig.8 b, c, d.

For the run out specimen with 500x100 μm micronotch, loaded at τ_a= 330 MPa, the non propagating crack deepest point is near to 110 μm deep, and for the run out specimens with

1000x100 µm micronotch, loaded at τ_a= 300 MPa, the maximum crack depth is 40-90 µm. This evidence shows the existence of a Mode III coplanar growth ahead of the micronotch. Using the results of the FEA, in particular the geometric factors of the cracks, it was possible to calculate SIF for the maximum depth of these coplanar cracks. The results showed that the ratio of $K_{III}/\Delta K_{I,th}$ is equal to one in the case of 500x100 µm micronotch, and for 1000x100 µm micronotch is equal to 1,4-1,35.

Two points are worth remarking: i) the crack size in this analysis of 'small cracks' is expressed by √area parameter by Murakami [10] and not by crack depth; ii) threshold is controlled by Mode I facets at the bottom of the micronotch since Mode III is predominant because of the micronotch shape (while for semi-circular cracks threshold is controlled by Mode II - Mode I branching at surface tips [4]). Moreover results tend to show a dependence on defect size similar to the one of Mode I [11].

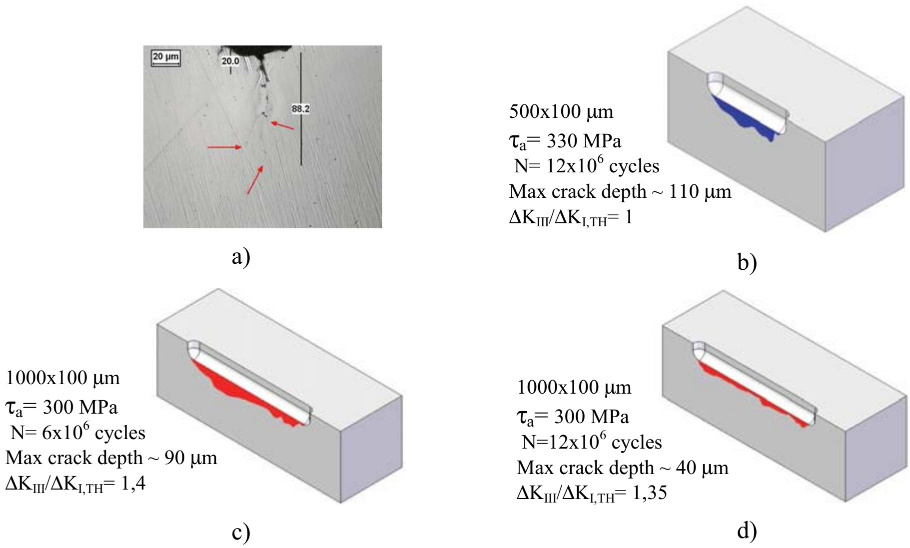

Fig.8. Results of the transverse sectioning of the run out specimens: a) image taken at about 440 µm from the micronotch tip(τ_a= 330 MPa N= 12x10^6 cycles); b), c), d) approximated crack front on run out specimens

Running elasto-plastic FEA, using tensile cyclic properties of the material (see Fig.9a), in particular the material cyclic behavior was modeled by Ramberg-Osgood relationship (E_{cyclic}= 204368 MPa, hardening coefficient H= 1598.9 MPa, hardening exponent n= 0.100925) [7], it was possible to estimate plastic radius in front of the hypothetical 20 µm non propagating crack. It can be seen that, considering the non propagating crack in order of 20 µm, Mode III crack have had a coplanar growth longer than plastic radius ahead of the micronotch.

Table 2. Results of the non-linear FEA

Micronotch type [length x depth]	1000x100 [µm]	500x100[µm]
$R_{p\,0.05}$ = 742 [MPa]	$\Delta\tau_w$ = 630 [MPa]	$\Delta\tau_w$ = 660 [MPa]
crack depth = 20 [µm]	plastic radius = 60 [µm]	plastic radius = 60 [µm]

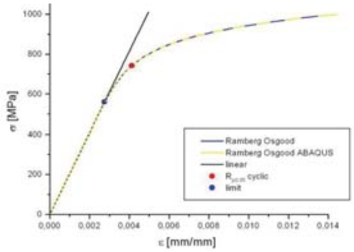

a)

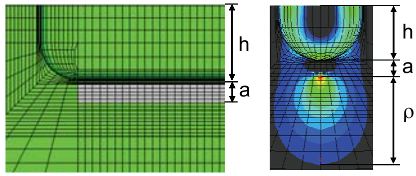

"h"-height of the micronotch; "a" - crack depth;

"ρ" - plastic radius

b)

Fig.9 Elasto-plastic analysis: a) properties of the material, Ramberg-Osgood curve; b) scheme of the crack FE modeling and yielded zone in the crack tip.

Concluding remarks

In this paper some experimental results about torsion fatigue strength in presence of shallow micronotches have been presented showing that: i) the ratio τ_w/σ_w is very different from the literature value for the round defects; ii) the shallow micronotches have a Mode III SIF almost constant for approximately 60% of the defect length; iii) Mode III shear cracks are triggered to propagate due to the presence of shallow micronotch, forming branches at 45° towards the end of the defect; iv) threshold is controlled by Mode I branches, but there is a competition with Mode III coplanar growth ahead of the micronotch.

Reference

[1] Y. Murakami, and M. Endo: Int. J. Fatigue, Vol. 16, 1994, p. 163-181.

[2] S. Beretta, and Y. Murakami: Fat. Fract. Engng. Mater. Struct., Vol. 23, 2000, p. 97-104.

[3] M. Endo: Trans. J. Soc. Mat. Sci. , Vol. 45, 1996, p. 16-20.

[4] Y. Murakami, and K. Takahashi: Fat. Fract. Engng. Mater. Struct., Vol. 21, 1998, p. 1473-1484.

[5] S. Beretta, in: Proceedings of the Europing Conference on Fracture (ECF14), Cracow, 2002.

[6] MK Kassir, GC Sih: E. J. Appl. Mech, Trans. ASME, Vol 33, 1966, p. 601-611.

[7] ABAQUS ver.6.5: reference manual(2005).

[8] M.Y. He & J.W. Hutchinson: Eng. Fract. Mech., Vol. 65, 2000, p. 1-14.

[9] L.P. Pook: Crack Paths, WitPress, Southampton, UK, 2002.

[10] Y. Murakami: Eng. Fract. Mech., Vol. 22, 1985, p. 101-114.

[11] S. Beretta, A. Cerrini, H. Desimone: Eng. Fract. Mech., Vol. 75, 2008, p. 845-856.